PAMUKKALE ÜNİVERSİTESİ
Mühendislik Bilimleri Dergisi

Araştırma makalesi | Research paper

PAMUKKALE UNIVERSITY
Journal of Engineering Sciences

Cilt | Vol: XX • Sayı | No: X • ss | pp: XXXX-XXXX • Yıl | Year: 20XX

One-dimensional non-isothermal modeling and parametric analysis of a hydrogen-based ammonia synthesis reactor

Yagmur Nalbant Atak

ARTICLE INFO

Dates:
Received: 02.04.2026
Accepted: 15.06.2026

Doi:
10.65206/pajes.1922045

Corresponding author:
Yagmur Nalbant Atak
(yagmur.atak@atilim.edu.tr)

Author addresses:
Department of Mechanical Engineering, Faculty of Engineering, Atılım University, Ankara, 06836, Türkiye
(yagmur.atak@atilim.edu.tr)

ABSTRACT

Context—Ammonia synthesis is a key process in the global chemical industry, especially for fertilizer production and emerging hydrogen-based energy systems. With growing interest in green hydrogen, ammonia has gained attention as both an energy carrier and a chemical feedstock. Therefore, understanding reactor behavior under different operating conditions is essential, and mathematical modeling provides an effective tool for analyzing performance and evaluating parameter effects without extensive experimental work.

Objective—The objective of this study is to develop a one-dimensional non-isothermal packed-bed reactor model for hydrogen-based ammonia synthesis and to evaluate the effects of key parameters, including inlet composition, pressure, and catalyst loading, on reactor performance.

Graphical representation of a one-dimensional non-isothermal packed-bed reactor model for hydrogen-based ammonia synthesis and key parametric findings.

Method—The model is based on species mass balances, an energy balance, and pressure drop described by the Ergun equation. The reaction kinetics were represented using the Temkin–Pyzhev rate expression, which is widely used for ammonia synthesis systems. The governing differential equations were solved numerically in MATLAB using an ODE solver. The model predicts the axial variation of temperature, pressure, molar flow rates, mole fractions, and the conversions of nitrogen and hydrogen along the reactor length. A parametric analysis was then performed by systematically varying inlet hydrogen–nitrogen composition, inlet pressure, and catalyst amount.

Results—Under the base operating conditions (T_{in} = 700 K, P_{in} = 35 bar, y_{H2} = 0.75, y_{N2} = 0.25, m_{cat} = 3 g, ε = 0.40), the model predicts outlet nitrogen and hydrogen conversions of approximately 0.1161, while the ammonia molar flow rate at the reactor outlet reaches 3.84 × 10^{-5} mol/s. The results show that ammonia formation increases along the reactor length due to the progress of the exothermic reaction. Among the investigated parameters, inlet pressure has the most pronounced effect on ammonia production. The highest formation was observed at an inlet pressure of 100 bar, where the outlet ammonia molar flow rate reached 9.02 × 10^{-5} mol/s and the nitrogen and hydrogen conversions increased to approximately 0.1500. The optimal feed composition within the investigated range was found near the stoichiometric ratio (y_{H2} = 0.75, y_{N2} = 0.25). Catalyst loading in the range of 1–5 g produced only minor changes in performance, with slightly higher ammonia production observed around 2–3 g.

Conclusion—In conclusion, the developed one-dimensional non-isothermal reactor model successfully describes the axial behavior of a hydrogen-based ammonia synthesis reactor and provides valuable insights into the influence of operating and bed parameters. Unlike many previous studies, the present work provides a simple integrated framework for evaluating the effects of operating and packed-bed parameters on hydrogen-based ammonia synthesis reactors.

Key Words—Ammonia production, Hydrogen-based processes, Non-isothermal modeling, Packed-bed reactor.

I. INTRODUCTION

Global energy demand is increasing day by day, and a significant part of this demand is still met by fossil fuels (e.g., coal and natural gas), leading to serious environmental concerns such as greenhouse gas emissions, global warming, and climate change. Due to these challenges, hydrogen has attracted considerable attention as a clean energy carrier due to its carbon-free nature and potential to support sustainable energy systems [1]. However, despite its advantages, hydrogen faces critical limitations related to storage and transportation, primarily due to its low volumetric energy density and the need for high-pressure or cryogenic conditions [2]. To overcome these limitations, alternative hydrogen carriers have been extensively investigated, among which ammonia has emerged as one of the most promising candidates [3] due to its high volumetric hydrogen density, well-established production technologies, and existing global infrastructure for storage and transportation, which enable its large-scale implementation in energy systems [4]. Recent studies have highlighted that ammonia can play a key role in the transition toward sustainable energy by enabling the storage, transport, and utilization of renewable hydrogen. For instance, Juangsa et al. [5] analyzed thermochemical and electrochemical ammonia production routes and emphasized their potential for sustainable hydrogen systems. Similarly, Kojima and Yamaguchi [6] evaluated the energy efficiency of ammonia compared to other hydrogen carriers such as liquid hydrogen and methylcyclohexane, showing that ammonia can offer competitive or superior performance. Furthermore, comprehensive review studies have demonstrated that ammonia provides advantages in terms of hydrogen storage density, infrastructure compatibility, and large-scale applicability [1], [2].

Given its growing significance, gaining a deeper understanding of ammonia synthesis processes and improving their performance has become increasingly important. In this regard, modeling and simulation studies of ammonia synthesis reactors offer a practical way to analyze reactor behavior and evaluate the influence of various operating conditions and design parameters [7]. Such approaches enable a systematic assessment of reactor performance and contribute to the optimization of reactor design, while reducing the reliance on extensive experimental work [8], [9]. For example, Shamiri and Aliabadi [10] studied the performance improvement of an industrial ammonia synthesis reactor using a heterogeneous model that incorporates diffusion–reaction effects through an effectiveness factor. Their results showed good agreement with industrial data, and by optimizing temperature profiles via quench valve adjustments, ammonia conversion increased from 15.26% to 15.45%, leading to a production increase of approximately 3 t/day and energy savings of 1.66 GJ/h. Additionally, temperature differences across the reactor increased, enhancing steam generation by about 2 t/h. Farsi et al. [11] studied the modeling and optimization of a commercial ammonia production process using a steady-state mathematical model that integrates reforming, shift conversion, and synthesis units. Their results showed that ammonia production could be increased from 1890 to 2179 mol/s (approximately 15%) by optimizing operating conditions such as feed temperature and reformer parameters. Additionally, improved energy utilization and hydrogen conversion efficiency were achieved, highlighting the strong impact of process conditions on overall ammonia production performance. Carvalho et al. [12] studied the modeling and optimization of an ammonia synthesis reactor using a penalty-like method combined with numerical techniques for solving nonlinear differential equations. Their results showed that reactor performance is highly sensitive to operating conditions such as feeding temperature, reactor length, and reactant partial pressures, and that optimization can significantly enhance ammonia production. The study reported an increase in ammonia conversion of approximately 10–15% under optimized conditions, along with improved concentration profiles along the reactor length. Palys et al. [13] studied the modeling and optimal design of an absorbent-enhanced ammonia synthesis process using a dynamic reactor model. Their work showed that ammonia synthesis could be carried out at significantly lower pressures (15–30 bar) compared to conventional Haber–Bosch conditions, while maintaining effective production performance. The results indicated that the synthesis loop accounts for approximately 20–25% of the total system capital cost, and that for production capacities below 6075 kg/h, the proposed process becomes economically more favorable than the conventional process, with cost scaling following a 0.77 capacity exponent. El-Shafie et al. [14] studied the kinetic modeling of ammonia synthesis using an integral reactor model based on the Langmuir–Hinshelwood mechanism under milder operating conditions. Their results showed good agreement with experimental data within an error range of ±20%, indicating high predictive capability of the developed model. In addition, increasing operating pressure significantly enhanced ammonia synthesis rates, with reported values reaching up to 29.6 mmol $h^{-1}g^{-1}$, highlighting the strong influence of pressure and catalyst performance on reactor efficiency.

Despite the extensive research on ammonia synthesis reactor modeling, many existing studies mainly focus on industrial-scale optimization, advanced reactor configurations, membrane-assisted systems, or catalyst-specific kinetic investigations. In addition, several studies evaluate only limited operating parameters under specific conditions. Although one-dimensional non-isothermal packed-bed reactor models are widely used in ammonia synthesis analysis, a clear and integrated evaluation of the combined effects of operating conditions and packed-bed parameters under hydrogen-based ammonia synthesis conditions remains relatively limited in literature. In particular, the simultaneous assessment of inlet pressure, feed composition, catalyst loading, axial temperature behavior, and pressure drop within a unified modeling framework has not been sufficiently emphasized in previous studies. Therefore, the present study aims to develop a simplified yet comprehensive one-dimensional non-isothermal packed-bed reactor model for hydrogen-based ammonia synthesis that incorporates mass, energy, and momentum balances together with Temkin–Pyzhev reaction kinetics and pressure-drop effects. Unlike studies focusing primarily on advanced reactor concepts or process-wide optimization, the present work emphasizes systematic reactor-level analysis and comparative parametric evaluation under consistent modeling assumptions.

The main contribution of this study is summarized as follows:

- Development of a unified non-isothermal reactor framework including coupled mass, energy, and momentum balances.
- Simultaneous investigation of the effects of inlet pressure, feed composition, and catalyst loading on reactor performance.
- Detailed analysis of axial reactor behavior, including temperature, pressure, molar flow rate, and conversion profiles.
- Provision of a computationally efficient engineering model suitable for reactor analysis, preliminary reactor design, and hydrogen-based ammonia synthesis studies.

Accordingly, this study provides a practical and systematic framework for understanding the interaction between reaction kinetics, thermodynamic limitations, and packed-bed reactor behavior in hydrogen-based ammonia synthesis systems.

II. MATHEMATICAL MODELING

In this study, ammonia synthesis is modeled as a one-dimensional, steady-state, non-isothermal, adiabatic packed-bed reactor. The ammonia synthesis reaction is given as in (1):

$$N_2 + 3H_2 \leftrightarrow 2NH_3. \quad (1)$$

The model was developed to describe the axial variation of species flow rates, temperature, and pressure along the reactor length. The mathematical formulation of reactor modeling combines species mass balances, an energy balance, and a pressure-drop equation. The complete set of governing differential equations was solved numerically in MATLAB program. To simplify the reactor analysis while preserving the main physical and chemical phenomena, the following assumptions were adopted:

- The reactor operates in a steady state.
- The reactor is one-dimensional, and only axial variations are considered.
- Radial gradients of temperature, concentration, and pressure are neglected.
- The gas phase behaves as an ideal gas.
- The catalyst bed is treated as a packed bed with uniform porosity.
- The reactor is adiabatic, and heat exchange with the surroundings is neglected.
- Catalyst deactivation is neglected.
- Internal and external mass transfer limitations are not explicitly considered.
- Gas viscosity and heat capacities are represented using simplified correlations suitable for engineering calculations.

Such assumptions are commonly used in ammonia reactor modeling studies and provide a reasonable approximation for packed-bed systems [15]. The geometrical and operating parameters used in the present model are summarized in Table 1. These parameters were selected based on literature data for laboratory-scale ammonia synthesis reactors and standard packed-bed reactor assumptions. Reactor dimensions, operating temperature and pressure, and feed composition were adopted from reported experimental studies, while bed porosity and particle size were chosen within commonly accepted ranges for packed-bed systems.

A. Species balance equations

The molar flow rate of each component changes along the reactor due to the ammonia synthesis reaction. For a packed-bed reactor, the species balances are written with respect to the axial position z as in (2)-(4):

$$dF_{N_2}/dz = -r_{N_2}(m_{Cat}/L), \quad (2)$$

$$dF_{H_2}/dz = -3r_{N_2}(m_{Cat}/L), \quad (3)$$

$$dF_{NH_3}/dz = 2r_{N_2}(m_{Cat}/L). \quad (4)$$

where F_i is the molar flow rate of component i, r_{N_2} is the reaction rate defined with respect to nitrogen consumption, m_{Cat} is the mass of catalyst, and L is the reactor length. The total molar flow rate at any axial position is calculated as:

Table 1. Geometrical and operating parameters used in the model.

Parameter / Description	Value/Unit	Ref.
Reactor length, L	0.15 m	[16]
Reactor diameter, D	0.006 m	[16]
Cross-sectional area, A_c	2.83×10^{-5} m^2	Calculated
Catalyst type	Ruthenium (Ru)-based catalysts	[17]
Catalyst mass, m_{cat}	0.003 kg	[16]
Particle diameter, d_p	1.0×10^{-3} m	[16]
Bed porosity, ε_b	0.40 [-]	[18]
Inlet temperature, T_{in}	700 K (673-773 K)	[17]
Inlet pressure, P_{in}	35 bar (10-50 bar)	[17]
H_2 mole fraction, y_{H_2}	0.75 [-]	[16]
N_2 mole fraction, y_{N_2}	0.25 [-]	[16]
Volumetric flow rate, Q_{H_2}	0.7×10^{-6} m^3/s	[16]

$$F_{tot} = F_{H_2} + F_{N_2} + F_{NH_3}. \quad (5)$$

The mole fractions of the components are then obtained by (6) as in the following:

$$y_i = F_i/F_{tot}. \quad (6)$$

These mole fractions are later used for the calculation of partial pressures, thermophysical properties, and conversion values.

B. Reaction kinetics

The ammonia synthesis rate was described using the Temkin–Pyzhev kinetic model [19], which is widely used for ammonia reactor analysis. The kinetic constants and corrected rate expressions used in this study were adopted from the work of Morud and Skogestad [7]. The rate expression employed in this work is given by (7):

$$r_{N_2} = f\left(k_1\left(P_{N_2}P_{H_2}^{1.5}\right)/P_{NH_3} - k_{-1}\,P_{NH_3}/P_{H_2}^{1.5}\right), \quad (7)$$

where f is the activity factor, k_1 is the forward rate constant, k_{-1} is the reverse rate constant, and p_i denotes the partial pressure of component i. The temperature-dependent rate constants are defined by (8) and (9) as follows [7]:

$$k_1 = 1.79\times10^4 e^{-87090/(RT)}, \quad (8)$$

$$k_{-1} = 2.57\times10^4 e^{-198464/(RT)}. \quad (9)$$

The partial pressures are calculated from the mole fractions and total pressure as in (10):

$$P_i = y_i P, \quad (10)$$

where the pressure is used in bar, consistent with the kinetic expression. In numerical implementation, the rate calculated from (7) is converted to $mol\times kg_{cat}^{-1}s^{-1}$.

C. Energy balance

Since the reactor is assumed to be adiabatic, the temperature change along the bed is governed only by the heat generated by the ammonia synthesis reaction. The energy balance is expressed by (11) as follows [20]:

$$dT/dz = -\left[\Delta H_{rxn} r_{N_2}(m_{Cat}/L)\right]/\left(F_{tot}C_{p,mix}\right), \quad (11)$$

where ΔH_{rxn} is the reaction enthalpy and $C_{p,mix}$ is the molar heat capacity of the gas mixture. The reaction is exothermic, and the standard enthalpy of formation [21] was taken as in (12):

$$\Delta H_{rxn} = 2x(-45.9) \cong -92\ kJ/mol. \quad (12)$$

The mixture heat capacity [22] was calculated from the component heat capacities and mole fractions using (13):

$$C_{p,mix} = y_{H_2}C_{p,H_2} + y_{N_2}C_{p,N_2} + y_{NH_3}C_{p,NH_3}. \quad (13)$$

For simplicity, the pure-component heat capacities were approximated by linear temperature-dependent correlations suitable for engineering calculations over the temperature range considered in this work. The simplified heat capacity correlations used in the code are defined by (14)-(16):

$$C_{p,H_2} = 28.8 + 1.0\times10^{-3}(T-300) \quad (14)$$

$$C_{p,N_2} = 29.0 + 3.0\times10^{-3}(T-300) \quad (15)$$

$$C_{p,NH_3} = 35.0 + 2.0\times10^{-2}(T-300) \quad (16)$$

where C_p is in $Jmol^{-1}K^{-1}$.

D. Pressure drop through the packed bed

The pressure drop along the catalyst bed was described as in (17) using the Ergun equation [23], which accounts for both viscous and inertial effects in packed beds:

$$dP/dz = -\left[150(1-\varepsilon_b)^2\mu u_s/\left(\varepsilon_b^3 d_p^2\right) + 1.75(1-\varepsilon_b)\rho_g u_s^2/\left(\varepsilon_b^3 d_p\right)\right] \quad (17)$$

where ε_b, d_p, μ, u_s and ρ_g indicate the bed porosity, particle diameter, gas viscosity, superficial velocity, and gas density, respectively. In the numerical implementation, pressure drop was first calculated in Pa/m and then converted to bar/m. This equation is particularly important for non-isothermal packed-bed systems because pressure affects both the gas density and the reaction rate through the partial pressures.

E. Auxiliary relations

The gas volumetric flow rate (Q) was calculated from the ideal gas law using (18):

$$Q = F_{tot}RT/P. \quad (18)$$

The superficial velocity was then obtained by (19):

$$u_s = Q/A_c. \quad (19)$$

The gas density was calculated using (20):

$$\rho_g = PMW_{mix}/(RT), \quad (20)$$

where the mixture molecular weight is defined by (21):

$$MW_{mix} = y_{H_2}MW_{H_2} + y_{N_2}MW_{N_2} + y_{NH_3}MW_{NH_3}. \quad (21)$$

The molecular weights for H_2, N_2, and NH_3 used were 2.016×10^{-3}kg/mol, 28.0134×10^{-3}kg/mol, 17.0305×10^{-3}kg/mol, respectively.

The gas viscosity was approximated by (22) as follows:

$$\mu = y_{H_2}\mu_{H_2} + y_{N_2}\mu_{N_2} + y_{NH_3}\mu_{NH_3} \quad (22)$$

with simplified temperature-dependent correlations defined by (23)-(25):

$$\mu_{H_2} = 9.0 \times 10^{-6}(T/300)^{0.7} \quad (23)$$

$$\mu_{N_2} = 1.8 \times 10^{-5}(T/300)^{0.7} \quad (24)$$

$$\mu_{NH_3} = 1.0 \times 10^{-5}(T/300)^{0.7} \quad (25)$$

where μ is in Pa ×·s.

F. Conversion definitions

The performance of the reactor was mainly evaluated in terms of nitrogen and hydrogen conversions. The nitrogen conversion was defined by (26):

$$X_{N_2} = \left(F_{N_2,in} - F_{N_2}\right)/F_{N_2,in} \quad (26)$$

Similarly, the hydrogen conversion was calculated using (27) as follows:

$$X_{H_2} = \left(F_{H_2,in} - F_{H_2}\right)/F_{H_2,in} \quad (27)$$

These definitions were used both for axial profiles and for outlet-based parametric comparisons.

G. Boundary conditions and numerical solution procedure

The developed reactor model consists of a system of coupled, nonlinear ordinary differential equations describing mass, energy, and momentum balances along the reactor length. These equations were solved numerically to obtain the axial profiles of species molar flow rates, temperature, and pressure.

1. Boundary conditions

The model was solved as an initial value problem, where all state variables were specified at the reactor inlet ($z = 0$). The inlet conditions are given as in (28):

$$F_{N_2}(0) = F_{N_2,0};\ F_{H_2}(0) = F_{H_2,0};\ F_{NH_3}(0) = F_{NH_3,0};$$
$$T(0) = T_0;\ P(0) = P_0 \quad (28)$$

These inlet values were varied parametrically to analyze the effect of operating conditions on reactor performance.

2. Numerical solution procedure

The numerical solution of the reactor model was carried out using a sequential axial integration approach. The governing mass, energy, and momentum balance equations were solved simultaneously along the reactor length by treating the system as an initial value problem. At each axial position, local thermophysical properties such as heat capacity, viscosity, and density were evaluated based on the instantaneous temperature, pressure, and composition. The reaction rate was then calculated using the Temkin–Pyzhev kinetic expression. Subsequently, the coupled differential equations were integrated to update the molar flow rates, temperature, and pressure. This procedure was repeated iteratively along the reactor length until the outlet conditions were obtained. The overall computational workflow is illustrated in Fig. 1.

III. RESULTS and DISCUSSION

The developed one-dimensional non-isothermal packed-bed reactor model was used to investigate the effects of key operating and bed parameters on ammonia synthesis performance. The reactor behavior was evaluated in terms of axial profiles of temperature, pressure, molar flow rates, and conversions of nitrogen and hydrogen, as well as ammonia production at the reactor outlet. In addition, a systematic parametric analysis was carried out by varying the inlet temperature, inlet pressure, inlet gas composition, and catalyst loading. The baseline operating conditions and the ranges of parameters considered in parametric analysis are summarized in Table 2.

A. Axial variation of reactor performance variables

The axial variation of temperature (Fig. 2a), pressure (Fig. 2b), molar flow rates (Fig. 2c), and hydrogen conversion (Fig. 2d) provides insight into the internal behavior of the packed-bed reactor. Analyzing these profiles is essential for understanding the complex interaction between reaction kinetics, heat effects, and pressure drop within the reactor. In particular, the temperature profile reflects the exothermic nature of the reaction, while the pressure profile indicates the influence of flow resistance through the packed bed. The variation in molar flow rates and conversion along the reactor length reveals the extent and location of reaction progress, allowing identification of regions where the reaction rate is highest or limited by thermodynamic equilibrium.

As shown in Fig. 2a, the reactor temperature increases rapidly from approximately 700 K at the inlet to about 770–775 K, corresponding to an increase of nearly 10–11% within the first 0.03–0.05 m of the reactor. This sharp temperature rise reflects

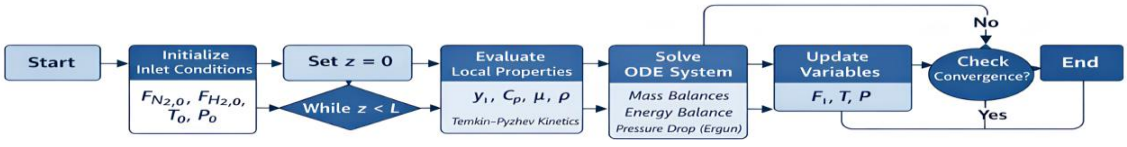

Fig. 1. Computational workflow of the coupled non-isothermal packed-bed ammonia synthesis reactor model including thermophysical property evaluation, reaction kinetics, mass balance, energy balance, and pressure-drop calculations.

Table 2. Baseline conditions and parameter ranges used in the study.

Parameter	Description	Baseline Value	Range Investigated
T_{in}	Inlet temperature	700 K	673 – 773 K
P_{in}	Inlet pressure	35 bar	10 – 50 bar
y_{H_2}	Hydrogen mole fraction	0.75	0.65 – 0.85
y_{N_2}	Nitrogen mole fraction	0.25	0.15 – 0.35
m_{cat}	Catalyst mass	3 g	1 – 5 g
ε_b	Bed porosity	0.40	0.30 – 0.60

the strong exothermic nature of the ammonia synthesis reaction. Beyond this region, the temperature profile becomes nearly constant, indicating that the reaction rate decreases as the system approaches thermodynamic equilibrium. Fig. 2b shows a slight pressure decrease from 35.0 bar to approximately 34.999 bar, corresponding to a negligible drop of less than 0.003% across the reactor. This minimal change indicates that pressure drop has a very limited influence on reactor performance under the conditions studied. The hydrogen conversion profile in Fig. 2c shows a rapid increase from 0 to approximately 0.09–0.095, meaning that nearly 9–9.5% of hydrogen is converted, with most of this conversion occurring within the first 0.04–0.05 m. After this point, the conversion remains nearly constant, indicating that the reaction becomes limited by equilibrium rather than kinetics. As shown in Fig. 2d, the mole fraction of ammonia increases from nearly zero to approximately 0.05–0.06, representing a significant relative increase in product formation along the reactor. In contrast, hydrogen decreases from about 0.75 to 0.70–0.71 (a decrease of approximately 5–7%), while nitrogen decreases from 0.25 to approximately 0.23–0.24 (a reduction of about 4–8%). These trends are consistent with the reaction stoichiometry and confirm the progressive formation of ammonia along the reactor length. According to the results, more than 80–90% of the total conversion is achieved within the first third of the reactor, indicating that the remaining reactor length contributes only marginally to additional ammonia production under the given operating conditions.

B. Effect of inlet temperature

Inlet temperature is one of the most critical parameters influencing ammonia synthesis in packed-bed reactors, as it directly affects both reaction kinetics and thermodynamic equilibrium. Increasing temperature enhances the reaction rate due to higher molecular activity, while simultaneously reducing the equilibrium conversion for this exothermic reaction. Therefore, understanding the effect of inlet temperature is essential for identifying optimal operating conditions that balance reaction rate and ammonia yield. Fig. 3a illustrates the effect of inlet temperature on the axial profile of ammonia molar flow rate. As shown, increasing the inlet temperature significantly affects both the rate of ammonia formation and the final ammonia production. At lower inlet temperature (673 K), the ammonia molar flow rate increases gradually along the reactor and reaches the highest outlet value of approximately 2.4 × 10^{-5} mol/s. In contrast, at higher inlet temperatures (700–773 K), ammonia formation occurs more rapidly near the reactor inlet. Still, the final outlet values are lower, reaching approximately 2.0 × 10^{-5} mol/s at 700 K, 1.7 × 10^{-5} mol/s at 723 K, and 1.2 × 10^{-5} mol/s at 773 K. This corresponds to a decrease of approximately 15–20%, 30%, and up to 50% in ammonia production when the inlet temperature is increased from 673 K to 700 K, 723 K, and 773 K, respectively. The results indicate that higher inlet temperatures enhance the initial reaction rate due to increased kinetic activity, as evidenced by the steeper profiles near the reactor inlet. However, because ammonia synthesis is an exothermic reaction, increasing temperature shifts the thermodynamic equilibrium toward the reactants, thereby reducing the maximum achievable concentration of ammonia. Consequently, although higher temperatures accelerate reaction rates, lower inlet temperatures favor higher ammonia yields

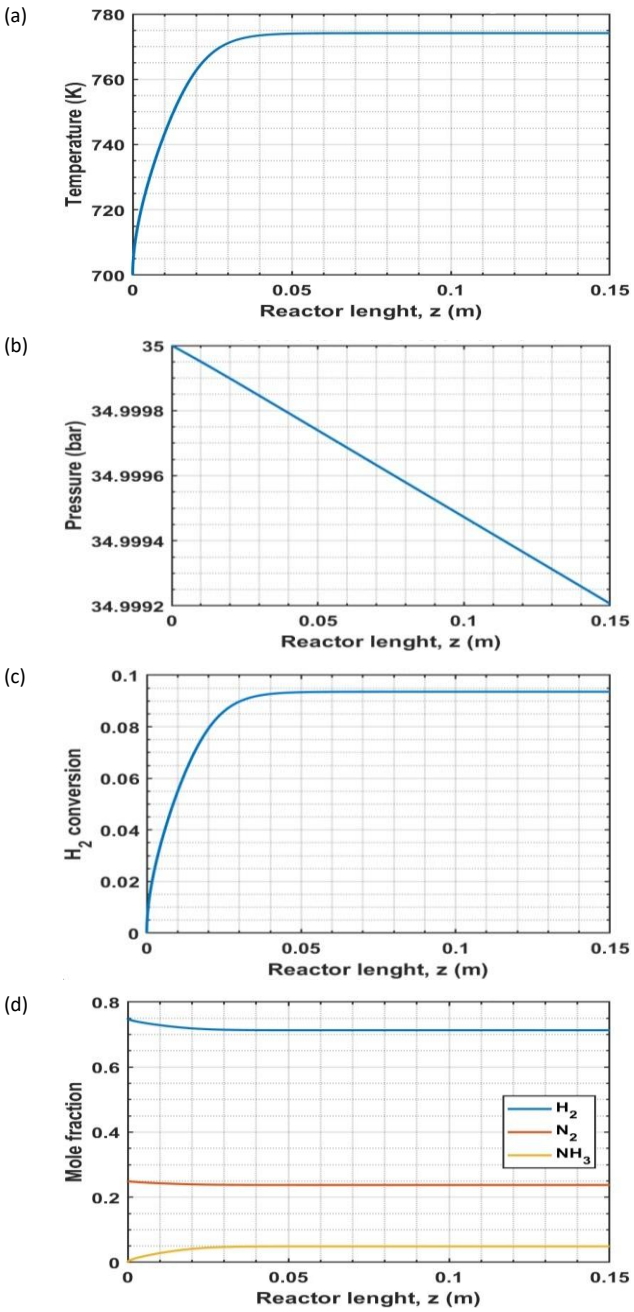

Fig. 2. Axial profiles of (a) temperature, (b) pressure, (c) molar flow rates, (d) hydrogen conversion along the packed-bed reactor.

under the studied conditions. This highlights the trade-off between reaction kinetics and thermodynamic equilibrium in ammonia synthesis. Fig. 3b shows the effect of inlet temperature on the outlet ammonia molar flow rate. As observed, ammonia production decreases monotonically with increasing inlet temperature. The highest ammonia production is obtained at 673 K, reaching approximately 2.4 × 10^{-5} mol/s, while increasing the inlet temperature to 700 K, 723 K, and 773 K reduces the outlet ammonia molar flow rate to approximately 2.0 × 10^{-5}, 1.7 × 10^{-5}, and 1.2 × 10^{-5} mol/s, respectively. This corresponds to a decrease of about 15–20% at 700 K, 30% at 723 K, and up to 50% at 773 K relative to the lowest temperature case. This trend clearly indicates that although higher temperatures enhance reaction kinetics, they significantly reduce ammonia yield due to the unfavorable shift in thermodynamic equilibrium for this exothermic reaction. Therefore, lower inlet temperatures are more favorable for maximizing ammonia production under the studied conditions. Hydrogen conversion is strongly influenced by inlet temperature due to its impact on both reaction kinetics and thermodynamic equilibrium. As shown in Fig. 3c, inlet

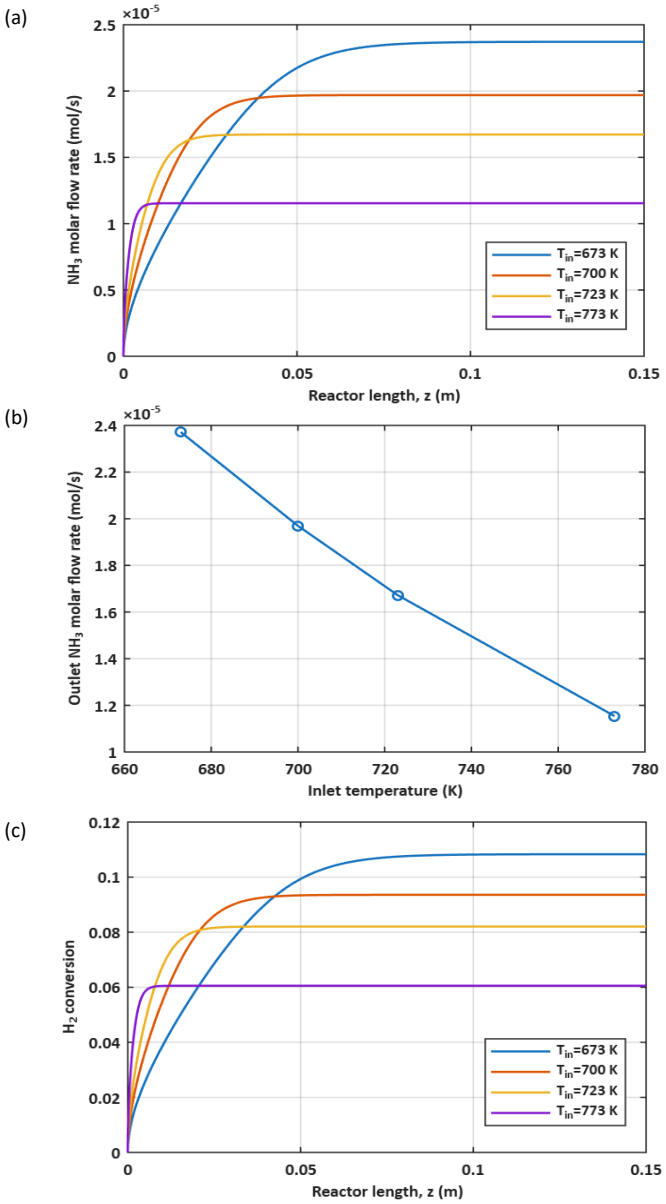

Fig. 3. Effect of inlet temperature on (a) the axial profile of ammonia molar flow rate, (b) outlet ammonia molar flow rate, (c) the axial profile of hydrogen conversion.

temperature has a significant effect on the axial profile of hydrogen conversion. At lower inlet temperature (673 K), the hydrogen conversion increases more gradually along the reactor length but reaches the highest final value of approximately 0.105–0.110. In contrast, at higher inlet temperatures (700–773 K), the conversion increases more rapidly near the reactor inlet, as indicated by the steeper initial slopes. However, the final conversion values are lower, reaching approximately 0.095 at 700 K, 0.082 at 723 K, and 0.060 at 773 K. This corresponds to a reduction of approximately 10–15%, 20–25%, and up to 40–45% in hydrogen conversion as the inlet temperature increases from 673 K to 700 K, 723 K, and 773 K, respectively. The results clearly show that higher temperatures enhance the reaction rate in the initial region of the reactor due to improved kinetics but reduce the overall conversion due to unfavorable thermodynamic equilibrium for this exothermic reaction. Therefore, lower inlet temperatures favor higher hydrogen conversion, while higher temperatures lead to faster but less efficient overall conversion.

C. Effect of inlet pressure

Inlet pressure is one of the most influential operating parameters in ammonia synthesis, as it directly affects both reaction equilibrium and reaction rate through changes in partial pressures. Since ammonia synthesis involves a reduction in the total number of gas moles, increasing pressure shifts the equilibrium toward ammonia formation. Therefore, analyzing the effect of inlet pressure is essential for understanding reactor performance and identifying favorable operating conditions. Fig. 4a illustrates the effect of inlet pressure on the axial profile of ammonia molar flow rate. As shown, increasing inlet pressure significantly enhances ammonia production throughout the reactor length. At the lowest pressure (10 bar), the outlet ammonia molar flow rate reaches approximately 0.25×10^{-5} mol/s, indicating very limited ammonia formation. Increasing the pressure to 20 bar raises ammonia production to approximately 0.8×10^{-5} mol/s, representing a substantial increase of more than threefold. Further increasing the pressure to 35 bar results in an outlet ammonia molar flow rate of approximately 2.0×10^{-5} mol/s, which is about 2.5 times higher than the 20 bar case and nearly eight times higher than the 10 bar case. At the highest pressure (50 bar), ammonia production reaches approximately $3.3–3.4 \times 10^{-5}$ mol/s, corresponding to an increase of about 65–70% compared to 35 bar and more than an order of magnitude higher than the 10 bar case. In addition to increasing the final ammonia yield, higher pressures also accelerate ammonia formation along the reactor length, as indicated by the steeper profiles near the reactor inlet. This behavior is attributed to the thermodynamic characteristics of the ammonia synthesis reaction, where increasing pressure shifts the equilibrium toward ammonia due to the decrease in the total number of gas moles. Moreover, higher pressure increases reactant partial pressures, thereby enhancing the reaction rate. Fig. 4b presents the variation of outlet ammonia molar flow rate as a function of inlet pressure. Unlike the axial profiles shown in Fig. 4a, this figure provides a direct comparison of reactor performance in terms of final ammonia production. As shown, ammonia production increases nonlinearly with increasing inlet pressure. The outlet ammonia molar flow rate rises from approximately 0.25×10^{-5} mol/s at 10 bar to about 3.3×10^{-5} mol/s at 50 bar, indicating a substantial improvement in reactor performance. The curvature of the trend suggests that the sensitivity of ammonia production to pressure becomes more pronounced at higher pressures. This indicates that operating at elevated pressures is particularly beneficial for maximizing ammonia yield. Therefore, this figure highlights the strong dependence of reactor performance on pressure and provides a clear basis for selecting optimal operating conditions. Fig. 4c shows the effect of inlet pressure on the axial profile of hydrogen conversion. As observed, hydrogen conversion increases significantly with increasing pressure, with higher pressures leading to both faster conversion near the reactor inlet and higher final conversion levels. At 10 bar, the hydrogen conversion reaches approximately 0.045, indicating limited reaction extent under low-pressure conditions. Increasing the pressure to 20 bar raises the conversion to approximately 0.070, corresponding to an increase of about 55–60%. Further increases in pressure to 35 bar and 50 bar result in hydrogen conversion values of approximately 0.093 and 0.110, respectively. This corresponds to an additional increase of about 30–35% from 20 to 35 bar and about 15–20% from 35 to 50 bar. Overall, the conversion at 50 bar is more than twice that at 10 bar. In addition to increasing the final conversion, higher pressures also shift the region of rapid conversion closer to the reactor inlet, indicating enhanced reaction rates under elevated pressure conditions. These results further confirm that increasing pressure improves reactor performance by promoting both higher reaction rates and greater equilibrium conversion.

D. Effect of catalyst amount

Catalyst amount is a key design parameter in packed-bed reactors, as it directly determines the number of available active sites for the reaction. Increasing the catalyst loading generally enhances the reaction rate by providing a larger surface area for reactant adsorption and reaction. However, beyond a certain

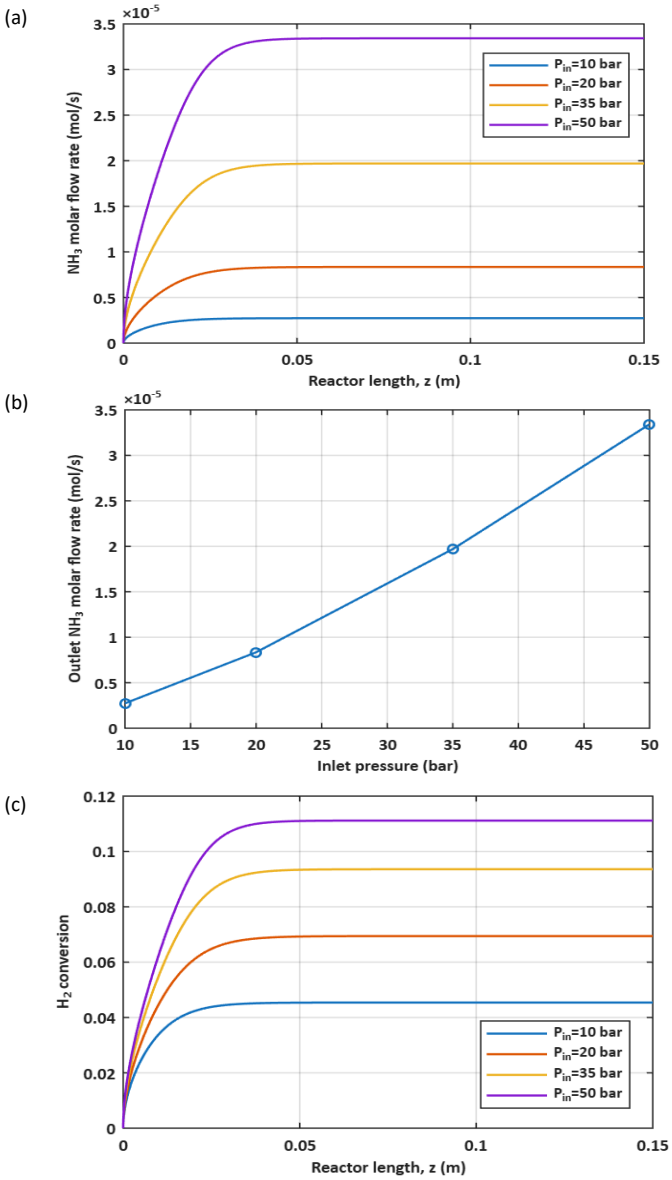

Fig. 4. Effect of inlet pressure on (a) the axial profile of ammonia molar flow rate, (b) outlet ammonia molar flow rate, (c) the axial profile of hydrogen conversion.

level, the effect of additional catalysts may become limited due to thermodynamic constraints or reduced reactant availability. Therefore, evaluating the effect of catalyst amount is essential for identifying optimal reactor design and operating conditions [25]. Fig. 5a illustrates the effect of catalyst amount on the axial profile of ammonia molar flow rate. As shown, increasing the catalyst amount accelerates ammonia formation along the reactor length, resulting in a steeper increase in ammonia molar flow rate near the reactor inlet. At the lowest catalyst loading (1 g), ammonia formation occurs more gradually, and the outlet ammonia molar flow rate approaches approximately 2.0×10^{-5} mol/s only after a longer reactor length. In contrast, increasing the catalyst amount to 3–5 g leads to a much faster approach to the same outlet value, with most of the ammonia being formed within the first 0.02–0.04 m of the reactor. This indicates that increasing catalyst loading significantly enhances the reaction rate, particularly in the initial region of the reactor. For example, increasing the catalyst amount from 1 g to 3 g reduces the required reactor length to reach near-maximum ammonia production by more than 50%. However, despite the noticeable differences in axial profiles, the final outlet ammonia molar flow rate remains nearly constant at approximately 2.0×10^{-5} mol/s for all catalyst amounts. This suggests that the reactor performance is ultimately limited by thermodynamic equilibrium rather than catalyst availability under the studied conditions. Therefore, increasing catalyst amount primarily improves the reaction rate and reduces the required reactor length, but has a negligible effect on the final ammonia yield. Fig. 5b presents the effect of catalyst amount on the outlet ammonia molar flow rate. Unlike the axial profiles shown in Fig. 5a, this figure directly compares the overall reactor performance in terms of final ammonia production. As observed, increasing the catalyst amount from 1 g to 2 g results in a slight increase in outlet ammonia molar flow rate, from approximately 1.965×10^{-5} mol/s to 1.969×10^{-5} mol/s, corresponding to an increase of less than 0.3%. Further increases in catalyst amount from 2 g to 5 g show virtually no change in ammonia production, with the outlet value remaining nearly constant at approximately 1.969×10^{-5} mol/s. This behavior clearly indicates that the reactor is operating close to thermodynamic equilibrium under the conditions studied, and that additional catalyst does not significantly enhance ammonia yield. Therefore, while increasing catalyst amount improves the reaction rate and reduces the required reactor length (as shown in Fig. 5a), it has a negligible effect on the final ammonia production. This suggests that an optimal catalyst loading exists, beyond which further increases are not economically justified. Fig. 5c shows the effect of catalyst amount on the axial profile of hydrogen conversion. As observed, increasing the catalyst amount significantly accelerates hydrogen conversion along the reactor length, particularly in the initial region of the reactor. At the lowest catalyst loading (1 g), hydrogen conversion increases gradually and reaches approximately 0.095 at the reactor outlet. In contrast, higher catalyst amounts (3–5 g) lead to a much faster increase in conversion, reaching similar final values within a significantly shorter reactor length. For example, increasing the catalyst amount from 1 g to 3 g reduces the reactor length required to achieve a conversion of 0.09 from approximately 0.10 m to about 0.03–0.04 m, corresponding to a reduction of nearly 60–70%. Further increasing the catalyst loading to 5 g reduces this required length even more, to less than 0.02–0.03 m, indicating an additional improvement of approximately 20–30%. Despite these significant differences in axial behavior, the final hydrogen conversion remains nearly constant for all catalyst amounts, with values ranging between 0.093 and 0.095, corresponding to a variation of less than 2–3%. This confirms that increasing catalyst amount primarily enhances the reaction rate and shifts the reaction zone toward the reactor inlet, while having a negligible effect on the final conversion due to thermodynamic limitations.

E. Qualitative and quantitative comparison with literature

To evaluate the reliability and accuracy of the developed model, the predicted results were compared with previously reported studies in the literature. Both qualitative trends and quantitative values were considered in the comparison, including temperature rise, conversion levels, ammonia production, and the effects of key operating parameters.

As summarized in Table 3, the model predictions fall within the ranges reported in the literature and exhibit similar behavioral trends. In particular, the predicted temperature increase, conversion levels, and pressure dependence of ammonia formation are in good agreement with previous studies. Minor deviations are expected due to differences in reactor configurations, operating conditions, and modeling assumptions. This comparison demonstrates that the developed model successfully captures the essential characteristics of ammonia synthesis in packed-bed reactors and can be considered reliable for parametric analysis and reactor performance evaluation.

It should be noted that the comparison is based on literature ranges, as exact matching operating conditions are not available. Differences may arise due to variations in reactor configurations, catalyst properties, and modeling approaches. In addition, the present model is based on several simplifying assumptions,

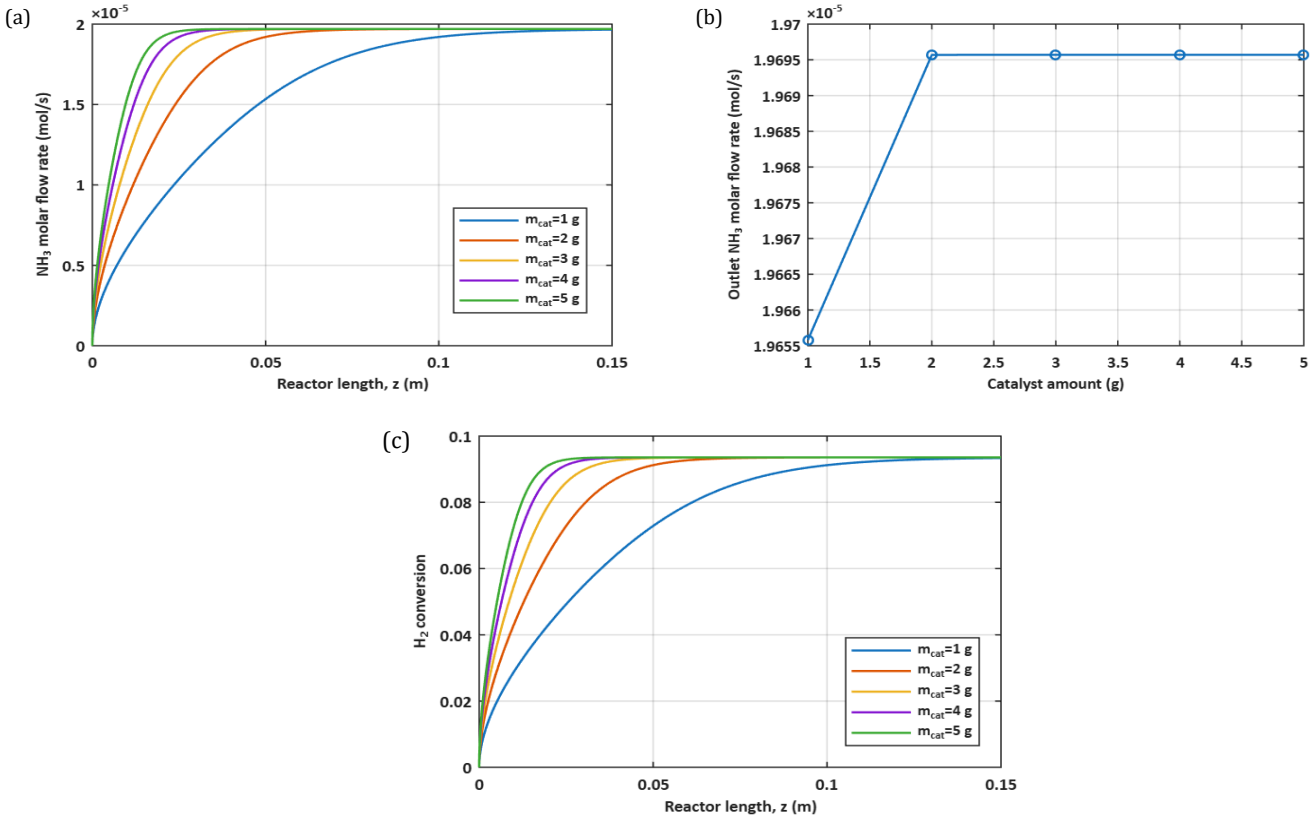

Fig. 5. Effect of catalyst amount on (a) the axial profile of ammonia molar flow rate, (b) outlet ammonia molar flow rate, (c) the axial profile of hydrogen conversion.

Table 3. Combined qualitative and quantitative comparison with literature.

Aspect	Present Study (Quantitative)	Present Study (Trend)	Literature (Quantitative / Trend)	Ref.
Temperature profile	ΔT ≈ 70–75 K	Rapid increase near inlet, then plateau	ΔT=50–100 K; similar exothermic behavior	[10], [12]
Conversion level	X ≈ 0.09–0.11	Conversion mainly in first reactor section	X = 0.08–0.15; similar trend	[11], [14]
NH_3 production	$\sim 10^{-5}$ mol/s	Increases along reactor, reaches plateau	10^{-5}–10^{-4} mol/s; comparable behavior	[11]
Pressure effect	~8–10× increase	Strong nonlinear increase with pressure	Pressure strongly enhances NH_3 formation	[14]
Catalyst effect	<3% variation in outlet	Affects rate, not final yield	Minor effect under equilibrium conditions	[11]
Reaction zone	First 20–30% of reactor	Reaction concentrated near inlet	Similar behavior in packed-bed reactors	[10], [12]

including one-dimensional flow, ideal gas behavior, and the neglect of mass transfer limitations and catalyst deactivation. These assumptions may influence the quantitative accuracy of the results, particularly under extreme operating conditions. Nevertheless, the model provides a reasonable representation of ammonia synthesis behavior and captures the key trends observed in the literature.

IV. CONCLUSION

In this study, a one-dimensional steady-state non-isothermal packed-bed reactor model for hydrogen-based ammonia synthesis was developed and solved numerically to analyze reactor performance under varying operating conditions. The model successfully captured the axial behavior of key variables, including temperature, pressure, molar flow rates, and reactant conversions, providing a detailed understanding of reactor dynamics. The main results are given as follows:

- Under base operating conditions (T = 700 K, P = 35 bar, yH_2 = 0.75, yN_2 = 0.25, mcat = 3 g, ε = 0.40), hydrogen conversion reached to ≈ 0.116 and outlet ammonia molar flow rate was 3.84×10^{-5} mol/s.
- The reaction is highly localized, approximately 80–90% of total conversion occurs within the first 20–30% of the reactor length.
- Temperature increased from 700 K to ~770–775 K (≈ 70–75 K rise) due to the exothermic reaction through the reactor length.
- The increasing pressure from 10 bar to 50 bar increased ammonia production by more than 10 times. In fact, the best performance (NH_3 flow rate = 9.02×10^{-5} mol/s and hydrogen conversion ≈ 0.150) was obtained at 100 bar.
- The decreasing inlet temperature from 773 K to 673 K increased NH_3 production by up to 50%.
- When the catalyst loading was increased from 1 to 5 g, the reaction rate increased significantly (reaction zone shortened by 60–70%), and outlet NH_3 production changed by < 3%, indicating equilibrium limitation.
- Predicted conversion (0.09–0.15) and NH_3 production (10^{-5}–10^{-4} mol/s) are consistent with literature.

The originality of the present study mainly lies in the integrated evaluation of operating conditions and packed-bed parameters within a unified non-isothermal ammonia synthesis reactor framework. Although the employed reactor formulation and Temkin–Pyzhev kinetics are well established in the literature, the present work provides a systematic comparative assessment of reactor behavior under hydrogen-based operating conditions by simultaneously considering reaction kinetics, heat effects, and pressure drop. Therefore, the developed model offers a practical and computationally efficient tool for engineering analysis and preliminary reactor performance evaluation.

Future studies may focus on improving the model by incorporating additional physical and chemical effects that were not considered in the present work. Furthermore, the model can be extended to investigate the integration of ammonia synthesis

with renewable energy systems. In such configurations, hydrogen can be produced via water electrolysis powered by renewable energy sources such as solar or wind energy and subsequently utilized in ammonia synthesis. This integrated approach has significant potential for enabling sustainable and low-carbon ammonia production. Future work may therefore include the coupling of the reactor model with electrolyzer systems and renewable energy inputs to evaluate system-level performance and optimization.

AUTHOR STATEMENT

Plagiarism Check—The article has been scanned with iThenticate and found to be compliant with the journal's plagiarism policy.
Conflict of Interest—There is no conflict of interest with any person/organization.
Ethics Committee Approval—Ethics committee approval is not required for this article.
Use of Artificial Intelligence Tools—Artificial intelligence tools were not used for content creation, data analysis, or scientific interpretation. AI-based tools (e.g., ChatGPT) were used for language editing, grammar correction, and improving the clarity of the manuscript, and to prepare the graphical abstract.
Funding—No institutional/financial support was received for this study.
Data availability—The data supporting the findings of this study was generated by the author and may be obtained from the author upon request.
CRediT Author Contribution—Conceptualization, Methodology, Software, Validation, Formal analysis, Investigation, Resources, Data Curation, Writing - Original Draft, Writing - Review & Editing, Visualization, and Supervision were all done by the author of the article.

REFERENCES

[1] D. K. Madheswaran, S. Vengatesan, S. Jegadheeswaran, M. Thangamuthu, H. Togun, B. Duraisamy, O. Y. Chun, M. W. Khan, "Ammonia as a hydrogen carrier: A comprehensive analysis of electrolysis efficiency and its potential in sustainable energy systems", *Renewable & Sustainable Energy Reviews*, 221, 115915, 2025. https://doi.org/10.1016/j.rser.2025.115915.

[2] M. Aziz, A. T. Wijayanta, A. B. D. Nandiyanto, "Ammonia as Effective Hydrogen Storage: A Review on Production, Storage and Utilization", *Energies*, 13(12), 3062, 2020. https://doi.org/10.3390/en13123062.

[3] M. Pinzón, R. García-Carpintero, A. R. de la Osa, A. Romero, D. Abad-Correa, P. Sánchez, "Ammonia as a hydrogen carrier: An energy approach", *Energy Conversion and Management*, 321, 118998, 2024. https://doi.org/10.1016/j.enconman.2024.118998.

[4] A. Valera-Medina, H. Xiao, M. Owen-Jones, W. I. F. David, P. J. Bowen, "Ammonia for power", *Progress in Energy and Combustion Science*, 69, 63-102, 2018. https://doi.org/10.1016/j.pecs.2018.07.001.

[5] F. B. Juangsa, A. R. Irhamna, M. Aziz, "Production of ammonia as potential hydrogen carrier: Review on thermochemical and electrochemical processes", *International Journal of Hydrogen Energy*, 46(27), 14455-14477, 2021. https://doi.org/10.1016/j.ijhydene.2021.01.214.

[6] Y. Kojima, M. Yamaguchi, "Ammonia as a hydrogen energy carrier", *International Journal of Hydrogen Energy*, 47(54), 22832-22839, 2022. https://doi.org/10.1016/j.ijhydene.2022.05.096.

[7] J. C. Morud, S. Skogestad, "Analysis of instability in an industrial ammonia reactor", *AIChE Journal*, 44(4), 888-895, 1998. https://doi.org/10.1002/aic.690440414.

[8] A. Dashti, K. Khorsand, M. A. Marvast, M. Kakavand, "Modeling and simulation of ammonia synthesis reactor", *Petroleum & Coal*, 48(2), 15-23, 2006.

[9] D. S. S. Jorqueira, A. M. B. Neto, M. T. M. Rodrigues, "Modeling and numerical simulation of ammonia synthesis reactors using compositional approach", *Advances in Chemical Engineering and Science,* 8(3), 124-143, 2018. https://doi.org/10.4236/aces.2018.83009.

[10] A. Shamiri, N. Aliabadi, "Modeling and performance improvement of an industrial ammonia synthesis reactor", *Chemical Engineering Journal Advances*, 8, 100177, 2021. https://doi.org/10.1016/j.ceja.2021.100177.

[11] M. Farsi, N. Chabi, M. R. Rahimpour, "Modeling and optimization of ammonia process: Effect of hydrogen unit performance on the ammonia yield", *International Journal of Hydrogen Energy*, 46(79), 39011-39022, 2021. https://doi.org/10.1016/j.ijhydene.2021.09.160.

[12] E. P. Carvalho, C. Borges, D. Andrade, J. Y. Yuan, M. A. S. S. Ravagnani, "Modeling and optimization of an ammonia reactor using a penalty-like method", *Applied Mathematics and Computation*, 237, 330-339, 2014. https://doi.org/10.1016/j.amc.2014.03.099.

[13] M. J. Palys, A. McCormick, E. L. Cussler, P. Daoutidis, "Modeling and optimal design of absorbent enhanced ammonia synthesis", *Processes*, 6(7), 91, 2018. https://doi.org/10.3390/pr6070091.

[14] M. El-Shafie, T. Yajima, T. Naito, K. Sato, S. Tsuda, K. Inazu, K. Nagaoka, Y. Kawajiri, "Comprehensive kinetic analysis of ammonia synthesis over a Co/BaO/MgO catalyst under milder conditions: Integral reactor modeling via Langmuir–Hinshelwood mechanism", *Chemical Engineering Journal*, 523, 168922, 2025. https://doi.org/10.1016/j.cej.2025.168922.

[15] I. Gargiulo, G. Anello, S. Richard, F. Gallucci, "Modeling of a packed bed membrane reactor for ammonia synthesis: on the role of membrane performance and operating conditions", *International Journal of Hydrogen Energy*, 166, 150995, 2025. https://doi.org/10.1016/j.ijhydene.2025.150995.

[16] M. Malmali, Y. M. Wei, A. McCormick, E. L. Cussler, "Ammonia synthesis at reduced pressure via reactive separation", *Industrial & Engineering Chemistry Research*, 55(33), 8922-8932, 2016. https://doi.org/10.1021/acs.iecr.6b01880.

[17] S. S. S. Ganti, P. K. Roy, N. Wagh, K. N. S. S. Sai, S. Kumar, "Strategically designed catalysts for ammonia synthesis under mild conditions: recent advances and challenges", *Journal of Materials Chemistry A*, 13(21), 15361-15426, 2025. https://doi.org/10.1039/D4TA08232J.

[18] D. Nemec, J. Levec, "Flow through packed bed reactors: 1. Single-phase flow", *Chemical Engineering Science*, 60(24), 6947-6957, 2005. https://doi.org/10.1016/j.ces.2005.05.068.

[19] A. Nielsen, J. Kjaer, B. Hansen, "Rate equation and mechanism of ammonia synthesis at industrial conditions", *Journal of Catalysis*, 3(1), 68-79, 1964. https://doi.org/10.1016/0021-9517(64)90094-6.

[20] H. S. Fogler, "Elements of chemical reaction engineering", 3rd Edition, Upper Saddle River, NJ, USA, Prentice-Hall Inc., 1999.

[21] P. Linstrom, "NIST Chemistry WebBook-SRD 69", National Institute of Standards and Technology, 2025. https://doi.org/10.18434/T4D303.

[22] J. M. Smith, H. C. Van Ness, M. M. Abbott, M. T. Swihart, "Introduction to chemical engineering thermodynamics", 9th Ed., Singapore, McGraw-Hill. 2022.

[23] S. Ergun, "Fluid flow through packed columns", *Chemical Engineering Progress*, 48(2), 89, 1952.

[24] G. F. Froment, K. B. Bischoff, J. De Wilde, "Chemical reactor analysis and design," 2nd Edition, New York – Chichester, USA, John Wiley & Sons, 1990, pp. 104-127.